



# Discovering phenotypic causal structure from nonexperimental data

Otsuka, Jun

---

**(Citation)**

Journal of Evolutionary Biology, 29(6):1268-1277

**(Issue Date)**

2016-06

**(Resource Type)**

journal article

**(Version)**

Accepted Manuscript

**(Rights)**

This is the peer reviewed version of the following article: [Journal of Evolutionary Biology, 29(6):1268-1277, 2016], which has been published in final form at <http://dx.doi.org/10.1111/jeb.12869>. This article may be used for non-commercial purposes in accordance with Wiley Terms and Conditions for Self-Archiving.

**(URL)**

<https://hdl.handle.net/20.500.14094/90003542>



Title: Discovering phenotypic causal structure from nonexperimental data

(Short title: Discovering phenotypic causal structure)

Author: Jun Otsuka

The Department of Philosophy

Kobe University

Rokko-dai 1-1, Nada, Kobe, Japan

Email: [junotk@gmail.com](mailto:junotk@gmail.com)

Phone: +81 (0)78 803-5502

Fax: +81 (0)78 803-5502

# Discovering phenotypic causal structure from nonexperimental data

## Abstract

The evolutionary potential of organisms depends on how their parts are structured into a cohesive whole. A major obstacle for empirical studies of phenotypic organization is that observed associations among characters usually confound different causal pathways such as pleiotropic modules, inter-phenotypic causal relationships, and environmental effects. The present article proposes causal search algorithms as a new tool to distinguish these different modes of phenotypic integration. Without assuming an a priori structure, the algorithms seek for a class of causal hypotheses consistent with independence relationships holding in observational data. The technique can be applied to discover causal relationships among a set of measured traits and to distinguish genuine selection from spurious correlations. The former application is illustrated with a biological dataset of rat morphological measurements previously analysed by Cheverud et al. (1983).

*Keywords: Natural selection, Quantitative genetics, Theory, Phenotypic integration, Causal models*

## Introduction

The developmental mechanism underlying phenotypic characters determines their variational properties and thus is instrumental in understanding the evolutionary potential. Darwin, in his discussion on ‘correlation of growth’, has emphasized that causal connections among distinct traits influence and sometimes constrain evolutionary changes. In the quantitative genetics literature, the study of constraints on adaptive evolution has focused on the additive genetic covariance matrix (the  $\mathbf{G}$  matrix) of the Lande equation  $\Delta\bar{\mathbf{z}} = \mathbf{G}\boldsymbol{\beta}$ . In particular, eigenvectors of  $\mathbf{G}$  associated with large eigenvalues are interpreted to point to directions to which adaptive response is less constrained (Arnold et al., 2001; Blows & Hoffmann, 2005; Blows, 2007; Walsh & Blows, 2009). Conversely, if one or more of the eigenvalues is zero, evolutionary trajectories are restricted onto a lower-dimensional hypersurface in the adaptive landscape, meaning there are phenotypic combinations unattainable by the population provided its  $\mathbf{G}$  matrix remains constant. Constraints in this context, therefore, are conceptualised as a restriction on the evolutionary trajectories of a population in the adaptive landscape. The  $\mathbf{G}$  matrix or its eigenstructure does not reveal the causal basis of constraints — it facilitates predicting *how* a population will respond to a given selective pressure, without explaining *why* on the physiological or developmental ground.

An alternative to this approach is to explicitly model the causal structure over phenotypic characters using a directed graph usually called a *path diagram* (Wright, 1920; Li, 1975; Lynch, 1988; Crespi & Bookstein, 1989;

Mitchell-Olds & Bergelson, 1990; Mitchell, 1992). For a set of  $n$  traits, a linear path model can be represented by an  $n \times n$  matrix whose  $ij$  element is the path coefficient of the  $i$ th trait on the  $j$ th trait, and is zero if there is no edge between them. A path analysis is usually used to model life history and distinguish indirect from direct fitness contributions of traits, with an aim to provide a more detailed picture of selection than that captured by selection gradient  $\beta$  that focuses solely on the proximate causes of fitness. Alternatively, a path model can be used to explicate the constraints summarized by the  $\mathbf{G}$  matrix in terms of direct causal relationships among phenotypes. Let  $\mathbf{B}$  be a matrix of the path coefficients for a given path diagram and define  $\Phi := (\mathbf{I} - \mathbf{B})^{-1}$  where  $\mathbf{I}$  is an identity matrix. Then the  $\mathbf{G}$  matrix can be written as:

$$\mathbf{G} = \Phi \mathbf{G}_\epsilon \Phi^T \quad (1)$$

where  $\mathbf{G}_\epsilon$  is the covariance of the additive genetic components *not* attributable to causal relationships among traits and the superscript T is a matrix transpose (Gianola & Sorensen, 2004; Morrissey, 2014; Otsuka, 2014). Inserting this into the Lande equation and re-arranging yields

$$\Delta \bar{\mathbf{z}} = \Phi \mathbf{G}_\epsilon \boldsymbol{\eta} \quad (2)$$

where the *extended selection gradients*  $\boldsymbol{\eta} := \Phi^T \beta$  measure the total (direct and indirect) effects of traits on the relative fitness (Morrissey, 2014).

Morrissey's equation (2) describes linear adaptive evolution as a function of selective pressures ( $\boldsymbol{\eta}$ ), the covariance of exogenous genetic values ( $\mathbf{G}_\epsilon$ ), and the phenotypic causal structure ( $\Phi$ ). To fit the model to an actual

population, however, one must first identify the path diagram, which is not a trivial task. The heuristic use of repeated multiple regression to construct a path diagram (Mitchell-Olds & Bergelson, 1990) is problematic for a regression coefficient inevitably confounds a direct causal relationship between traits with genetic associations (Kempthorne, 1978). Confirming a causal link with a manipulative experiment or assuming it on an a priori ground does not solve the issue because it does not eliminate the possibility of genetic confounding that may bias the estimation of the path coefficient. In general, a phenotypic correlation may arise in multiple, nonexclusive manners — by one trait causing the other, two traits sharing common environmental, genetic, or phenotypic causes, linkage disequilibrium, and sheer chance. Equation (2) requires one to manage these possible sources of phenotypic associations; however, no regression method can achieve this owing to insufficient degrees of freedom (Cowley & Atchley, 1992). Further, the construction of a path diagram presupposes the orientation of each causal edge; however, such an asymmetry can never be read off from correlation, which by nature is a symmetric relation.

Confounding also represents a serious obstacle in evolutionary predictions based on Lande’s equation, for one of its vital assumptions is that selection gradients  $\beta$  reflect all and only direct causal contributions from the phenotype to fitness, free from any unobserved environmental, phenotypic, or genetic confounding (Mitchell-Olds & Shaw, 1987; Hadfield, 2008; Morrissey et al., 2010). This cannot be guaranteed by the regression method alone. In another context, the  $\mathbf{G}$  matrix has been used, not only as a statistical summary of evolutionary potential but also to infer the underlying

genetic architecture or developmental *modules* (e.g., Atchley, 1984; Riska, 1986; Cheverud, 1996; Hansen, 2006; Hansen & Houle, 2008; Polly, 2008). A variety of methods have been proposed to detect a modular structure from genetic or phenotypic correlations (e.g., Cheverud and Buikstra, 1981; Cheverud et al., 1983; Phillips & Arnold, 1999; Mezey et al., 2000; Magwene, 2001, 2008; Mitteroecker & Bookstein, 2007, 2008; Zelditch, 1988), many of which are variants of the exploratory or confirmatory factor analysis. The underlying assumption of the factor analysis, and other proposals, to study genetic modules is that all phenotypic associations derive from pleiotropic genes and there are no horizontal (phenotypic) causal relations. This assumption, again, remains untested by these statistical methods.

Hence, identifying the causal structure of an evolving population proves both essential and challenging in either approach. The difficulty is familiar with the dictum ‘correlation is not causation’ — statistical information underdetermines causal relationships. Although this is true in general, recent decades have seen rapid developments of causal search algorithms that attempt to infer causal facts from statistical data (Pearl, 2000; Spirtes et al., 2000). Rather than directly fitting free parameters of an a priori model, these algorithms exploit patterns of conditional independence to reduce a candidate set of causal hypotheses consistent with the observed data. A reduction in the hypothesis space facilitates the determination of what model to fit with the data quantitatively. Although the causal modelling has been applied in ecology (Shipley, 2000, 2010) and the breeding literature (Valente et al., 2010, 2011; Rosa et al., 2011), its implication to the study of evolution and the relative significance vis-a-vis the existing methods are not well

documented. The present article aims to address this deficiency. Following a brief introduction of the basic idea of causal search, this article explores its potential in identifying a path model and distinguishing genuine selection from spurious correlations. Using the data reported by Cheverud et al. (1983) as input, it is demonstrated that the algorithm creates an ontogenetic process model that corresponds well with their findings. The method presented herein, however, is not a ‘silver bullet.’ The last section discusses its limitation and precautions in biological applications.

## **Constraint-based causal search**

### **Theoretical background**

The goal of causal search is to construct a path diagram from observational data, with no or minimum assumptions regarding a specific form of the causal structure to be identified. This is contrasted with traditional modelling practices that aim to quantitatively estimate parameters of some known or assumed structure. The search task consists of determining the presence or absence of a direct causal connection (adjacency) for each pair of variables and orienting causal edges. This section describes, in some detail, how the search algorithm manages these two subtasks. A more complete treatment can be found in Spirtes et al. (2000) or Pearl (2000). For an accessible introduction to biological contexts, see Shipley (2000, 2010).

The basic idea of causal search is that a probability distribution is generated from the underlying causal structure, and as such contains some trace of the latter in the form of conditional independence. As an example, sup-



Figure 1: Example of collider where two edges  $X_2 \rightarrow X_4$  and  $X_4 \leftarrow X_3$  collide at  $X_4$ .

pose Fig. 1 represents the true causal structure underlying four observed variables  $\{X_1, X_2, X_3, X_4\}$ . Then  $X_4$  will be probabilistically dependent on its remote cause  $X_1$ ; however, this dependence is cleared when conditioned upon the intermediates  $X_2$  and  $X_3$ ; in formal notation,  $X_1 \not\perp_p X_4$  and  $X_1 \perp_p X_4 | \{X_2, X_3\}$  where  $\perp_p$  denotes probabilistic independence and  $\not\perp_p$  dependence. The generative structure thus constrains possible forms of distribution in such a manner that probabilistic (in)dependence between variables suggests their causal (in)dependence. The notion of causal independence is more formally defined by *d-separation* (Pearl, 1988, 2000). A path  $p$  is said to be *d-separated* by a set of variables  $\mathbf{Z}$  if

1.  $p$  contains a chain  $i \rightarrow m \rightarrow j$  or a fork  $i \leftarrow m \rightarrow j$  such that the middle variable  $m$  is in  $\mathbf{Z}$ , or
2.  $p$  contains a collider  $i \rightarrow m \leftarrow j$  such that the middle variable  $m$  or any of its causal descendants is not in  $\mathbf{Z}$ .

We also say that variables  $X$  and  $Y$  are *d-separated* by  $\mathbf{Z}$  if every path between  $X$  and  $Y$  is *d-separated* by  $\mathbf{Z}$ , and denote this as  $X \perp_d Y | \mathbf{Z}$ .

Note that conditional independence ( $\perp_p$ ) is a probabilistic notion that can be tested vis-a-vis observed data, whereas *d-separation* ( $\perp_d$ ) is a topological feature of an unknown path diagram. A distribution is called *Markov*

with respect to a given path diagram if  $d$ -separation relationships in the latter entail probabilistic independence holding in the former, such that  $\mathbf{X} \perp_d \mathbf{Y} | \mathbf{Z} \Rightarrow \mathbf{X} \perp_p \mathbf{Y} | \mathbf{Z}$  for any choice of variables  $\mathbf{X}$ ,  $\mathbf{Y}$ , and  $\mathbf{Z}$ . When the opposite direction holds (probabilistic dependence implies  $d$ -separation), the distribution is called *faithful* or *stable*.

When do these two conditions hold? The Markov condition requires that any variable that affects more than one variable in the dataset be also measured, that is, there is no confounding. Suppose in the previous example,  $X_1$  and  $X_4$  were confounded by a latent variable. Then, they would no longer become independent even conditioned on the observed intermediates (i.e.,  $X_1 \not\perp_p X_4 | \{X_2, X_3\}$ ), despite they are  $d$ -separated (i.e.,  $X_1 \perp_d X_4 | \{X_2, X_3\}$ ) in the original diagram that omits the confounder. Because such confounding is expected to be the rule rather than the exception with phenotypic records, the Markov condition can hardly be assumed in the present context.

Faithfulness, conversely, is violated when there are multiple causal pathways whose effects cancel each other. In Fig. 1, this occurs when two pathways  $X_1 \rightarrow X_2 \rightarrow X_4$  and  $X_1 \rightarrow X_3 \rightarrow X_4$  exert the opposite influences such that the net effect of  $X_1$  on  $X_4$  is zero. If the system is linear, this occurs exactly when  $\beta_{41|2} = -\beta_{41|3}$ , where  $\beta_{41|k}$  is the partial regression coefficient of  $X_4$  on  $X_1$  given  $X_k$ ,  $k \in \{2, 3\}$ . Although not impossible, one may expect such a fine-tuned cancellation to be unlikely (Spirtes et al., 2000), and even if it occurs, it would not remain invariant under slight changes in the parameters (Pearl, 2000).

The causal search algorithm described below assumes faithfulness but

not the Markov property of an input distribution. The algorithm consists of three parts, adjacency, orientation, and follow-up. The first step of the algorithm constructs a non-directed graph that represents what variable is causally connected to another. Under the faithfulness assumption, an observed probabilistic independence implies the pair of variables to be  $d$ -separated. Using this property, the adjacency step determines, for any pair of variables in the dataset, whether they are causally disconnected by testing their conditional independence. More precisely,

1. For each pair of variables  $X$  and  $Y$ , find a set of variables  $\mathbf{S}(X, Y)$  (possibly empty) such that  $X \perp_p Y | \mathbf{S}(X, Y)$ . Connect  $X$  and  $Y$  with an undirected edge if and only if there is no such set.

Provided all statistical decisions of independence are made correctly, this rule yields an *adjacency graph* in which the *absence* of an edge between a pair of variables guarantees that they do not cause each other directly nor have a latent common cause. However, without the Markov condition the *presence* of an edge does not necessarily represent a direct causal relationship — it only means they are inseparably correlated, and this association may be due to a confounding factor.

Given an adjacency graph, the next step is to orient its undirected edges. The orientation process makes use of a specific structure called *collider* where two edges ‘collide’ at the middle node such that  $X \rightarrow Z \leftarrow Y$  (see the second part of the definition of  $d$ -separation). A unique property of the collider is that the variables at both ends ( $X, Y$ ) become *dependent* conditioned on the middle ( $Z$ ). For example the collider  $X_2 \rightarrow X_4 \leftarrow X_3$  in

Fig. 1 yields  $X_2 \perp_p X_3 | X_1$  but also  $X_2 \not\perp_p X_3 | \{X_1, X_4\}$ . An illustration of collider in the context of evolution is the linkage disequilibrium induced by selection, where selection creates a correlation between two uncorrelated loci  $L_1$  and  $L_2$  both affecting fitness  $W$ . In such cases  $L_1 \rightarrow W \leftarrow L_2$  forms a collider and conditioning on  $W$  by selection induces a genetic correlation. Colliders whose two ends are not connected to each other directly are called *unshielded*. Of course we do not know which part of a given adjacency graph forms a collider, or even an unshielded collider. But since only unshielded colliders can produce the unique pattern of independence just described, one can infer colliding points, and thus orient edges around them, based on the results of statistical tests. Using a wildcard symbol ‘\*’ to represent either the arrowtail ‘-’ or the head ‘>’, the second rule for edge orientation is:

2. For each triplet  $X, Z, Y$  such that  $X$  is adjacent to  $Z$ ,  $Z$  is adjacent to  $Y$ , and  $X$  is *not* adjacent to  $Y$ , orient  $X**Z**Y$  as  $X**\rightarrow Z \leftarrow *Y$  if and only if  $Z$  is not in  $\mathbf{S}(X, Y)$ .

Because all the unshielded colliders in the true graph must be identified by this rule, the remaining ternary relationships can be further oriented such that they do not create a new unshielded collider:

3. If there is a subgraph  $X**\rightarrow Y**Z$  with  $X$  and  $Z$  being nonadjacent, orient this as  $X**\rightarrow Y**\rightarrow Z$ .

Finally, if we can assume that the true causal structure is *acyclic* or *recursive*, that is, if no variable causes itself, the following rule is applicable:

4. If there is a directed path from  $X$  to  $Y$  where each edge is pointing

towards  $Y$  and they are directly connected by an edge  $X**Y$ , orient the edge as  $X*\rightarrow Y$ .

Otherwise,  $X$  and  $Y$  form a cycle and are causes of themselves, contrary to the assumption of acyclicity.

These rules are implemented by the FCI (Spirtes et al., 2000) and IC\* (Pearl, 2000) algorithms. From a sample distribution summarized by a covariance matrix or cell counts, these algorithms output a *partial ancestor graph* or PAG, which may contain four types of edges with the following meanings (Spirtes et al., 1995):

- $X \rightarrow Y$ :  $X$  causes  $Y$ . It may or may not be confounded.
- $X \leftrightarrow Y$ :  $X$  does not cause  $Y$  nor does  $Y$  cause  $X$ , however, they are confounded by a latent factor.
- $X \circ \rightarrow Y$ :  $X \rightarrow Y$  or  $X \leftrightarrow Y$ , however, the algorithm could not determine which is the case.
- $X \circ \circ Y$ : A causal relationship is suspected between  $X$  and  $Y$ , however, the algorithm could not determine its form.

There are two caveats in interpreting directed edges in a PAG. First, although an edge  $X \rightarrow Y$  implies  $X$  to be a cause of  $Y$ , the relation may be *indirect*, that is, the causal influence of  $X$  on  $Y$  may be mediated by other variables in the dataset. Further, directed edges, in general, do not exclude possible confounding factors, i.e., although  $X \rightarrow Y$  indicates  $X$  to be a cause of  $Y$ , they may further be confounded by other unobserved factors. There are, however, cases where such possibilities can be eliminated, as we will see

below. These complications do not arise under the Markov condition, i.e., when there is no confounding variable.

Fig. 2 illustrates an application of the above rules. The true causal structure is on the left, with  $\{X_1, X_2\}$  and  $\{X_3, X_4\}$  being confounded by latent factors. In distributions faithful to this graph, the pairs of variables  $\{X_1, X_4\}$  and  $\{X_2, X_3\}$  are independent given  $X_2$  and  $X_1$ , respectively (i.e.,  $X_1 \perp_p X_4|X_2$  and  $X_2 \perp_p X_3|X_1$ ), which enables the first step of the algorithm to build the adjacency graph (b). The same pairs, however, become dependent when conditioned on different variables,  $X_3$  and  $X_4$ , respectively ( $X_1 \not\perp_p X_4|X_3$  and  $X_2 \not\perp_p X_3|X_4$ ). These facts are used in Step 2 to identify the unshielded colliders  $X_1 * \rightarrow X_3 \leftarrow * X_4$  and  $X_2 * \rightarrow X_4 \leftarrow * X_3$  in the PAG (c). The third and fourth rules are not applicable in this example, leaving the remaining edges undetermined (denoted by the empty circles). Although the result is partial, this example illustrates that some facts regarding the underlying causal structure can be learned from statistical data alone. More can be inferred if the time order of variables is known, as we will see below.

Figure 2: Illustration of the causal discovery algorithm with the (in)dependence relationships used in each step of inference. (a) True causal structure with confounding (curved bi-directed edges). (b) Adjacency graph obtained after Step 1. (c) PAG obtained after Step 2. Open circles indicate where the algorithm could not determine the direction of causal influence.

## Causal search with the mixed model

As mentioned above, the majority of phenotypic records cannot be assumed to satisfy the Markov condition owing to genetic or environmental confounding. However, once these factors are statistically eliminated, one can search their causal structure by using algorithms that use both the faithfulness and Markov assumptions. This approach was proposed by Valente et al. (2010, 2011) who combine a causal search with the standard mixed model. A linear path model for a trait vector  $\mathbf{z}$  with random additive genetic effects  $\mathbf{u}$  and residual deviations  $\mathbf{e}$  can be written as

$$\begin{aligned}\mathbf{z} &= \mathbf{B}\mathbf{z} + \mathbf{X}\boldsymbol{\beta} + \mathbf{u} + \mathbf{e} \\ &= \Phi\mathbf{X}\boldsymbol{\beta} + \Phi(\mathbf{u} + \mathbf{e})\end{aligned}\tag{3}$$

where  $\mathbf{B}$  is a path coefficient matrix,  $\mathbf{X}$  is a design matrix,  $\boldsymbol{\beta}$  is a vector of fixed effects, and  $\Phi := (\mathbf{I} - \mathbf{B})^{-1}$  as defined above. Under the standard assumptions of the multi-trait mixed model (e.g.,  $\mathbf{u}$  and  $\mathbf{e}$  are normally distributed and independent of each other), the phenotypic covariance matrix is

$$\begin{aligned}\text{Var}(\mathbf{Z}) &= \Phi \text{Var}(\mathbf{U})\Phi^T + \Phi \text{Var}(\mathbf{E})\Phi^T \\ &:= \mathbf{G} + \mathbf{R}.\end{aligned}\tag{4}$$

Valente et al. (2010) note that  $\mathbf{G}$  and  $\mathbf{R}$  are the additive genetic and residual covariance matrices estimated by a mixed model. In particular, the residual component contains information regarding the phenotypic causal structure

$(\Phi)$ , and thus serves as an input to a causal search algorithm. If  $\text{Var}(\mathbf{E})$  is diagonal, the conditional (residual) distribution  $P(\mathbf{Z}|\mathbf{u})$  satisfies the Markov condition even if the unconditional  $P(\mathbf{Z})$  does not, which allows one to use a more powerful search algorithm such as the IC or PC algorithm (Pearl, 2000; Spirtes et al., 2000). The parameters of the obtained path model can then be estimated using Bayesian Markov Chain Monte Carlo method (Gianola & Sorensen, 2004; Valente et al., 2010, 2011).

This approach will be particularly effective under pervasive genetic associations, which may hide direct causal relationships among phenotypes. The advantage is balanced by increased standard errors in the estimated residual covariances, which may impair statistical decisions of independence. Moreover, the mixed model approach is inapplicable to observational field studies that lack pedigree information or cannot dismiss the possibility of environmental confounding. The FCI algorithm described above proves useful in such observational studies or even in designed experiments where some form of nongenetic confounding is suspected or cannot be discarded.

## Applications

### Inferring a developmental structure

This section illustrates the causal search algorithm described above with empirical data reported in Cheverud et al. (1983). Based on a longitudinal growth study of 561 cross-fostered rats (Atchley & Rutledge, 1980), Cheverud and colleagues estimated additive genetic, maternal, and residual covariance matrices for the log-transformed body weight measured at ages



14, 28, 42, 56, 70, and 189 days. Their study also reported estimated matrices for age-specific tail length; however, in this paper we discuss only the body weight data because they indicated similar results.

The causal connections among the six ontogenetic stages were explored using the FCI algorithm in the TETRAD software version 4.3.10-7 (available at <http://www.phil.cmu.edu/projects/tetrad/>). Assuming normality as in the original study, Fisher’s  $z$  was used to test independence:

$$z = \frac{\sqrt{n - |\mathbf{C}| - 3}}{2} \ln \left( \frac{1 + r_{XY.\mathbf{C}}}{1 - r_{XY.\mathbf{C}}} \right)$$

where  $n$  is the sample size and  $r_{XY.\mathbf{C}}$  is the sample partial correlation of  $X$  and  $Y$  given  $\mathbf{C}$ . If the population correlation is zero,  $z$  is asymptotically standard normal (Anderson, 2003). In each test independence was declared at the 95% significance level; however, the overall results remained robust at the 99% level. In addition to the reported matrices, background knowledge regarding the time order of the measurements was used to restrict possible directions of causal flow.

Fig. 3 (a) is the output of the FCI algorithm applied to the phenotypic correlation matrix of the six weight measurements. As expected, the result indicates a sequential causal path (straight edges), with some possible connections between distant stages (curved edges). As noted earlier, however, these curved edges in the PAG do not necessarily imply direct causal relationships; rather, they may reflect genetic or environmental confounding. For example, the curved edge  $W_{70} \rightarrow W_{189}$  only indicates that the weight at day 70 affects the weight at day 189 *in some manner* — the influence may

Figure 3: PAGs obtained from the FCI algorithm applied to the rat-measurement data in Cheverud et al. (1983). (a) Output from the phenotypic correlation matrix, which suggests linear pathways with possible causal influences over distant stages (curved edges). (b) Causal search on the residual matrix confirms that the phenotypic casual structure is sequential. (c) Results indicate that the curved edges in (a) reflect not a direct relationship, rather a genetic confounding (solid bi-directed edges). Dashed edges indicate possible genetic confounding (bi-directed, curved), inter-phenotypic causation (directed, straight), and environmental confounding (dotted, curved), respectively.

or may not be direct, i.e., it may simply reflect an indirect causal influence through  $W_{56} \rightarrow W_{70} \rightarrow W_{189}$ , with some confounding in-between.

To clear the remaining uncertainties, the FCI algorithm was reapplied to the residual correlation matrix, which amounts to the partial correlation matrix conditioned on additive genetic components and thus is free from additive genetic confounding (Valente et al., 2010). The output PAG indicates a straight linear pathway (Fig. 3 (b)) with a possible confounding only between  $W_{14}$  and  $W_{24}$ . The result suggests that all the curved edges in Fig. 3 (a) do not represent direct causal links, rather are artifacts of genetic confounding.

Furthermore, Fig. 3 (b) allows us to conclude the absence of significant environmental confounding for the stages later than  $W_{28}$ . To see this, suppose the edge  $W_{42} \rightarrow W_{56}$  is confounded. Then,  $W_{42}$  would be the middle point both of a collider  $W_{28} \rightarrow W_{42} \leftrightarrow W_{56}$  and a chain  $W_{28} \rightarrow W_{42} \rightarrow W_{56}$ , which means no set could make  $W_{28}$  and  $W_{56}$  independent (because if a set

contains  $W_{28}$ , the collider is not  $d$ -separated, whereas if it does not, the chain is not  $d$ -separated). However, if that were the case, they must be connected by Step 1 of the algorithm, contrary to the actual output. We can thus conclude that the edge  $W_{42} \rightarrow W_{56}$  is not confounded. As noted earlier, edges in a PAG are consistent with confounding in general; however, the possibility can be excluded if there is an additional causal input ( $W_{28}$  in this case) to the cause variable. Such additional variables are called *instrumental variables*. In our example, all variables other than  $W_{189}$  serve as instrumental variables in the PAG Fig. 3 (b) to clear the unconfoundedness of the edges later than  $W_{28}$ .

Fig. 3 (c) summarizes the above results. Recall that the curved edges in graph (a) suggest either direct causal links or confounding of environmental or genetic origin. The first two possibilities, however, are eliminated by the output from the residual correlation matrix (b), leaving genetic confounding to be the only consistent explanation. By reversing the above reasoning of instrumental variables, genetic confounding of  $W_{70}$  and  $W_{189}$  makes  $W_{70}$  the middle point of both a collider and a chain. This means they are dependent conditioned on any phenotypic variable, and thus connected in graph (a). For the same reason, the curved edge  $W_{28} \rightarrow W_{56}$  in (a) was induced by genetic confounding between  $W_{42}$  and  $W_{56}$ . The solid bi-directed edges at the bottom of graph (c) denote these genetic confounders. Conversely, the dashed edges represent the remaining uncertainties due primarily to the unavailability of instrumental variables at the early stages. If the individual phenotypic records and pedigree information are known (which are no longer available for the present data; James Cheverud, personal communication),

the path and genetic correlation coefficients of model Fig. 3 (c) can be estimated using the Bayesian MCMC technique mentioned above (Gianola & Sorensen, 2004)

The obtained causal graph suggests that the early development of rat body weight is controlled by age-specific growth factors rather than global pleiotropic effects. This hypothesis is consistent with the subsequent study on mice conducted by Cheverud et al. (1996) who found age-specific body weights of mice to be affected by distinct QTLs at different chromosomal locations, with few QTLs affecting postnatal growth as a whole. In the sequential pathway, the phenotypic effect of a single QTL would be detectable for only a limited time period owing to diminishing autocorrelation. The autocorrelation model also explains the observation made by both the original and subsequent studies that associations between age-specific weights decline as the time interval increases in all (phenotypic, genetic, maternal, and residual) correlation matrices (Cheverud et al., 1983, 1996). We thus conclude that the causal hypothesis obtained from the search algorithm was not only consistent with the input data but also extrapolatable to a further study.

### Identifying selective pressures

The issue of confounding also appears significant in empirical studies of selection (Lande & Arnold, 1983). It is well known that the ordinary least square estimate  $\hat{\beta}$  of selection gradients may be biased in the presence of unconditioned genetic, phenotypic, or environmental confounding factors (Mitchell-Olds & Shaw, 1987; Rausher, 1992; Mauricio & Mojonner, 1997;

Hadfield, 2008; Morrissey et al., 2010). If an unmeasured environmental factor  $X$  affects both phenotype  $Z_1$  and fitness  $W$ , regressing  $W$  on  $Z_1$  yields a nonzero  $\hat{\beta}_1$  even if there is no selection. Moreover, if  $Z_1$  is causally affected by or shares genetic or environmental common causes with another trait  $Z_2$  the estimate  $\hat{\beta}_2$  of its selection gradient is also biased because the multiple regression amounts to conditioning on the colliding point of  $Z_2 \rightarrow Z_1 \leftrightarrow W$  or  $Z_2 \leftrightarrow Z_1 \leftrightarrow W$  (Table 1, first and second rows). Hence, a confounding factor on only one trait may affect the entire selection estimators. The bias manifests itself as a discrepancy between the regression slopes of fitness on the focal traits and those on their breeding values and thus is detectable by comparing these two estimates (Rauscher, 1992; Queller, 1992; Morrissey et al., 2010, 2012). Such consistency tests, however, require phenotypic records of the offspring generation and therefore do not serve the purpose of predicting evolutionary responses.

Although there exists no infallible method to detect environmental confounders, under certain conditions it is possible to distinguish genuine selection from confounding based on the method of instrumental variables discussed above. An instrumental variable in the present context is an auxiliary trait that (1) causes or is genetically or environmentally confounded with the focal trait; but (2) does *not* directly cause nor is confounded with the fitness measure ( $Z_2$  in Table 1). The first condition is met by any trait previous in time that has a nonzero phenotypic correlation with the focal trait. Under the faithfulness assumption, a sufficient condition for the second requirement is the trait being independent of the fitness measure given some (possibly empty) set.

Let  $Z_2$  be such a trait, and  $\mathbf{S}(Z_2, W)$  be the set that renders  $Z_2$  independent of the fitness (i.e.,  $Z_2 \perp_p W | \mathbf{S}(Z_2, W)$ ). The test then declares  $Z_1$  free from confounding if and only if  $Z_1$  is included in  $\mathbf{S}(Z_2, W)$ . The rationale for the rule is as follows. If  $Z_1$  is confounded,  $Z_2 \ast \rightarrow Z_1 \leftrightarrow W$  forms an unshielded collider. Then, because  $Z_2$  and  $W$  would be dependent given  $Z_1$ , the set  $\mathbf{S}(Z_2, W)$  cannot contain  $Z_1$ . Conversely, if  $Z_2$  is not confounded, the only possibilities are  $Z_2 \leftrightarrow Z_1 \rightarrow W$  or  $Z_2 \rightarrow Z_1 \rightarrow W$  because the fitness cannot be a cause of a phenotype. In either case  $Z_2$  and  $W$  are dependent unless conditioned on  $Z_1$ , hence  $Z_1 \in \mathbf{S}(Z_2, W)$ . Table 1 illustrates this with bivariate cases.

The test requires no more than the standard significance test of selection gradients, i.e., a distribution must be faithful and allow independent tests. Upon determining the set of unconfounded phenotypes, their selection gradients can be estimated by regressing the fitness only on such a subset.

## Discussion

The evolutionary response of a population to selection is a function of its causal structure and genetic variances (Otsuka, 2015, in press). Owing to the inherent difficulty and/or limited feasibility of a manipulative experiment, however, our knowledge on organismal architectures and selective regimes must often rely on some or another form of statistical analyses. The common issue in nonexperimental studies is that a phenotypic correlation confounds genetic associations, environmental effects, and a direct causal relationship between phenotypes (Kempthorne, 1978; Cowley & Atchley, 1992). The

present article proposed a new approach to discern these three sources of statistical associations based on differential patterns of conditional independence. Unlike other model fitting-approaches such as factor analysis or path analysis, the inference algorithms do not rely on a particular assumption on the form of the unknown causal structure; rather, they make use of general conditions regarding the relationship between causality and probability.

The key assumption of the FCI algorithm used in this paper is faithfulness, which requires that any active (not  $d$ -separated) causal link yield a statistical dependence, or by contraposition, that independence entails  $d$ -separation. In practice, however, the algorithm requires a stronger assumption that a causal relationship must yield a *significant* association to trim the edges based upon the nonsignificant results of independence tests (Zhang & Spirtes, 2003). Therefore, the absence of an edge in an output graph does not warrant a conclusion of causal unrelatedness; rather, it reflects the fact that the statistical test did not detect a significant total effect. The qualification is especially imminent in the causal inference of life history traits where various types of trade-off are expected. If, for example, negatively correlated traits are positively selected, the trade-off among the fitness components may lead to an almost unfaithful distribution, which invites Type II errors and consequent incorrect edge omissions. The risk can be reduced by using a more inclusive variable set or increasing the sample size. No finite sample size, however, can guarantee that the probability of overlooking an existing causal influence is less than a given threshold, because any causal search procedure for confounded data is only *pointwise consistent* but not *uniformly consistent* (Robins et al., 2003). That is, we

do not know how powerful our test must be to detect a causal relationship because the effect in question can be arbitrarily small (i.e., almost unfaithful). Thus, although the FCI algorithm can correctly judge the adjacency at the asymptotic limit, no finite sample can be guaranteed to approximate this result. This limitation is not peculiar to the algorithm; rather, it applies to every nonexperimental method including regression and other statistical tests.

Whereas Type II errors result in edge omissions, Type I errors — mistakenly rejecting independence hypotheses — lead to incorrect edge commissions. Given that the algorithm involves repeated tests, there would be a non-negligible probability of making incorrect statistical decisions even with a reasonably high significance level, say 95% or 99%. The overall error probability of the algorithm is difficult to evaluate because (i) tests are not independent of each other; (ii) an incorrect statistical decision may be offset by subsequent tests without affecting the final output; (iii) conversely, one error may have multiple consequences, e.g., yielding incorrect adjacency and orientation; and all of these depend on the unknown causal structure (Spirtes et al., 2000, p. 96). It is possible, however, to control the false discovery rate of the adjacency step of the algorithm such that the expected proportion of the falsely discovered links to all those discovered is curbed under the user-specific value (Li & Wang, 2009).

Hence similar to any other statistical method, the output from the algorithm must not be accepted as a solid fact; rather, as a hypothesis for further experimental studies. Provided these caveats, causal modelling provides a promising approach to build, identify, and examine a causal hypothesis from



observational data. The emphasis on the model construction is what distinguishes causal search from the conventional statistical methods that focus on model fitting. Because these model assumptions remain basically untested, the estimated parameters frequently present a misleading picture regarding the biology of the organisms under study. The above discussed study of Cheverud et al. (1983), for example, identified two major principal components in the estimated  $\mathbf{G}$  matrix, which they interpreted as two modules of pleiotropic genes with distinct causal roles — the first group regulating the height of the growth curve and the second its shape. Such global pleiotropic effects, however, were not confirmed by the subsequent study (Cheverud et al., 1996) or the present reanalysis. Rather, the two principal components are likely to be artefacts resulting from the sequential ontogenetic pathway. Because the upstream stages mainly determine the intercept of the growth curve and the later stages regulate its slope, genetic variances at these different stages may have been detected as principal components each associated with the curve height on one hand and its shape on the other. If this is the case, the detected ‘components’ do not point to distinct biological mechanisms. In general, reification of principal components as genetic modules assumes the absence of inter-phenotypic causal relationships, whereas the causal interpretation of path coefficients estimated by path analysis or structural equation modelling is valid only if there is no genetic or environmental confounding. The method described in this paper can serve as an ante or post hoc check of the causal assumptions of these statistical models as well as of a biological interpretation of their result.

Another possible area of application is the study of selection. Despite

its crucial importance in understanding adaptive evolution, most empirical studies have paid relatively little attention to the possible bias in the estimated selection gradients due to unobserved confounders (Mitchell-Olds & Shaw, 1987; Rausher, 1992; Mauricio & Rausher, 1997; Hadfield, 2008; Morrissey et al., 2010). Although selection and spurious correlation are indistinguishable from a correlation alone, they generate distinctive patterns of conditional independence that can be tested with the aid of an instrumental trait variable. In addition, a violation of faithfulness in this context is less likely because it only happens when an unobserved fitness contribution of the auxiliary trait cancels the statistical dependence that arises from conditioning on the collider, and there is no biological reason to expect this to occur. To repeat, this does not imply impossibility, but given the scarcity of alternatives the method provides a useful tool to verify the bias of evolutionary predictions with fewer assumptions than the conventional regression analysis.

## Conclusions

A major obstacle for observational studies of phenotypic integration or selection is that statistical associations among traits or fitness are presumably confounded by multiple unknown factors. The present article described a causal search algorithm that exploits patterns of conditional independence to discern direct causal relationships between phenotypes from genetic or environmental confounding and to determine the direction of causal influence using the property of unshielded colliders. The method was illustrated

with the growth data of rats reported in Cheverud et al. (1983) and its application to distinguish selection from spurious correlation was suggested with a hypothetical example. The causal hypothesis obtained from the rat data provided a mechanistic explanation of the observed patterns of pleiotropy consistent with the common understanding of the ontogenetic sequence and a subsequent study (Cheverud et al., 1996). In combination with subsequent confirmatory experiments, the causal search algorithm can provide valuable information for furthering our understanding of the generative structure of phenotype and its implication to adaptive evolution.

## Acknowledgement

I am grateful to Jeremy Berg, James Cheverud, Brandon Cooper, Bruce Glymour, Clark Glymour, James Griesemer, Michael Morrissey, and anonymous reviewers for helpful comments on earlier versions of the manuscript. I also thank Graham Coop, Steve Sterns, and Günter Wagner for discussions. The author has no conflict of interest to declare. A part of this study was supported by the Japan Society for the Promotion of Science Grant-in-Aid for Postdoctoral Fellows (25-659).

## References

- Anderson, T. W. 2003. *An introduction to multivariate statistical analysis*, 3rd edn. Wiley, Hoboken, New Jersey.
- Arnold, S. J., Pfrender, M. E. & Jones, A. G. 2001. The adaptive landscape

as a conceptual bridge between micro- and macroevolution. *Genetica*, 112-113:9–32.

Atchley, W. R. 1984. Ontogeny, timing of development, and genetic variance-covariances structure. *Am. Nat.*, 123(4):519–540.

Atchley, W. R. & Rutledge, J. J. 1980. Genetic components of size and shape. I. Dynamics of components of phenotypic variability and covariability during ontogeny in the laboratory rat. *Evolution*, 34(6):1161–1173.

Blows, M. W. 2007. A tale of two matrices: multivariate approaches in evolutionary biology. *J. Evol. Biol.*, 20(1):1–8.

Blows, M. W. & Hoffmann, A. A. 2005. A reassessment of genetic limits to evolutionary change. *Ecology*, 86(6):1371–1384.

Cheverud, J. M. 1996. Developmental integration and the evolution of pleiotropy. *Integr. Comp. Biol.*, 36(1):44–50.

Cheverud, J. M. & Buikstra, J. 1981. Quantitative genetics of skeletal non-metric traits in the rhesus macaques on Cayo Santiago. II. Phenotypic, genetic, and environmental correlations between traits. *Am. J. Phys. Anthropol.*, 54:51–58.

Cheverud, J. M., Routman, E. J., Duarte, F. A. M., van Swinderen, B., Cothran, K. & Perel, C. 1996. Quantitative trait loci for murine growth. *Genetics*, 142:1305–1319.

Cheverud, J. M., Rutledge, J. J. & Atchley, W. R. 1983. Quantitative ge-

netics of development: genetic correlations among age-specific trait values and the evolution of ontogeny. *Evolution*, 37(5):895–905.

Cowley, D. & Atchley, W. R. 1992. Quantitative genetic models for development, epigenetic selection, and phenotypic evolution. *Evolution*, 46(2):495–518.

Crespi, B. J. & Bookstein, F. L. 1989. A path-analytic model for the measurement of selection on morphology. *Evolution*, 43(1):18–28.

Gianola, D. & Sorensen, D. 2004. Quantitative genetic models for describing simultaneous and recursive relationships between phenotypes. *Genetics*, 167:1407–1424.

Hadfield, J. D. 2008. Estimating evolutionary parameters when viability selection is operating. *Proceedings of the Royal Society B: Biological Sciences*, 275:723–734.

Hansen, T. F. 2006. The evolution of genetic architecture. *Annu. Rev. Ecol. Evol. Syst.*, 37(1):123–157.

Hansen, T. F. & Houle, D. 2008. Measuring and comparing evolvability and constraint in multivariate characters. *J. Evol. Biol.*, 21(5):1201–1219.

Kempthorne, O. 1978. Logical, epistemological and statistical aspects of nature-nurture data interpretation. *Biometrics*, 34:1–23.

Lande, R. & Arnold, S. J. 1983. The measurement of selection on correlated characters. *Evolution*, 37(6):1210–1226.

- Li, C. 1975. *Path analysis-a primer*. Boxwood Press, Pacific Grove, California.
- Li, J. & Wang, Z. 2009. Controlling the false discovery rate of the association/causality structure learned with the PC algorithm. *J. Mach. Learn. Res.*, 10:475–514.
- Lynch, M. 1988. Path analysis of ontogenetic data. In: *The dynamics of size-structured populations* (L. Persson & B. Ebenman, eds), pp. 29–46. Springer-Verlag, Berlin.
- Magwene, P. M. 2001. New tools for studying integration and modularity. *Evolution*, 55(9):1734–1745.
- Magwene, P. M. 2008. Using correlation proximity graphs to study phenotypic integration. *Evol. Biol.*, 35(3):191–198.
- Mauricio, R. & Mojonner, L. 1997. Reducing bias in the measurement of selection. *Trends Ecol. Evol.*, 12(11):433–436.
- Mauricio, R. & Rausher, M. D. 1997. Experimental manipulation of putative selective agents provides evidence for the role of natural enemies in the evolution of plant defense. *Evolution*, 51(5):1435–1444.
- Mezey, J. G., Cheverud, J. M. & Wagner, G. P. 2000. Is the genotype-phenotype map modular? A statistical approach using mouse quantitative trait loci data. *Genetics*, 156(1):305–311.
- Mitchell, R. J. 1992. Testing evolutionary and ecological hypotheses using path analysis and structural equation modelling. *Funct. Ecol.*, 6:123–129.

- Mitchell-Olds, T. & Bergelson, J. 1990. Statistical genetics of an annual plant, *Impatiens capensis*. II. Natural selection. *Genetics*, 124(2):416–421.
- Mitchell-Olds, T. & Shaw, R. G. 1987. Regression analysis of natural selection: statistical inference and biological interpretation. *Evolution*, 41(6):1149–1161.
- Mitteroecker, P. & Bookstein, F. L. 2007. The conceptual and statistical relationship between modularity and morphological integration. *Syst. Biol.*, 56(5):818–836.
- Mitteroecker, P. & Bookstein, F. L. 2008. The evolutionary role of modularity and integration in the hominoid cranium. *Evolution*, 62(4):943–958.
- Morrissey, M. B. 2014. Selection and evolution of causally covarying traits. *Evolution*, 68(6):1748–61.
- Morrissey, M. B., Kruuk, L. E. & Wilson, A. 2010. The danger of applying the breeder’s equation in observational studies of natural populations. *J. Evol. Biol.*, 23(11):2277–2288.
- Morrissey, M. B., Parker, D. J., Korsten, P., Pemberton, J. M., Kruuk, L. E., & Wilson, A. J. 2012. The prediction of adaptive evolution: empirical application of the secondary theorem of selection and comparison to the breeder’s equation. *Evolution*, 66(8):2399–2410.
- Otsuka, J. 2014. *The causal structure of evolutionary theory*. PhD thesis, Indiana University.

- Otsuka, J. 2015. Using causal models to integrate proximate and ultimate causation. *Biol. Philos.*, 30(1):19–37.
- Otsuka, J. in press. Causal foundations of evolutionary genetics. *Brit. J. Philos. Sci.*, doi: 10.1093/bjps/axu039.
- Pearl, J. 1988. *Probabilistic reasoning in intelligent systems: networks of plausible inference*. Morgan Kaufmann, San Francisco, California.
- Pearl, J. 2000. *Causality: models, reasoning, and inference*. Cambridge University Press, New York, New York.
- Phillips, P. C. & Arnold, S. J. 1999. Hierarchical comparison of genetic variance-covariance matrices. I. Using the flury hierarchy. *Evolution*, 53(5):1506–1515.
- Polly, P. 2008. Developmental dynamics and G-Matrices: can morphometric spaces be used to model phenotypic evolution? *Evolutionary biology*, 35(2):83–96.
- Queller, D. C. 1992. Quantitative genetics, inclusive fitness, and group selection. *Am. Nat.*, 139(3):540–558.
- Rausher, M. D. 1992. The measurement of selection on quantitative traits: biases due to environmental covariances between traits and fitness. *Evolution*, 46(3):616–626.
- Riska, B. 1986. Some models for development, growth, and morphometric correlation. *Evolution*, 40(6):1303–1311.



- Robins, B. J. M., Scheines, R., Spirtes, P. & Wasserman, L. 2003. Uniform consistency in causal inference. *Biometrika*, 90(3):491–515.
- Rosa, G., Valente, B. & De los Campos, G. 2011. Inferring causal phenotype networks using structural equation models. *Genet. Select. Evol.*, 43(6).
- Shipley, B. 2000. *Cause and correlation in biology: a user's guide to path analysis, structural equations and causal inference*. Cambridge University Press, New York, New York.
- Shipley, B. 2010. *From plant traits to vegetation structure: chance and selection in the assembly of ecological communities*. Cambridge University Press, Cambridge, UK.
- Spirtes, P., Glymour, C. & Scheines, R. 2000. *Causation, prediction, and search*, 2nd edn. The MIT Press, Cambridge, Massachusetts.
- Spirtes, P., Meek, C. & Richardson, T. 1995. Causal inference in the presence of latent variables and selection bias. In: *Proceedings of the Eleventh conference on Uncertainty in artificial intelligence* (P. Besnard & S. Hanks, eds), pp. 499–506, Morgan Kaufmann, San Francisco, California.
- Valente, B., Rosa, G., De los Campos, G., Gianola, D. & Silva, M. A. 2010. Searching for recursive causal structures in multivariate quantitative genetics mixed models. *Genetics*, 185(2):633–644.
- Valente, B. D., Rosa, G. J. M., Silva, M. A., Teixeira, R. B. & Torres, R. A. 2011. Searching for phenotypic causal networks involving complex traits: an application to European quail. *Genet. Select. Evol.*, 43(37).

- Walsh, B. & Blows, M. W. 2009. Abundant genetic variation + strong selection = multivariate genetic constraints: a geometric view of adaptation. *Annu. Rev. Ecol. Evol. Syst.*, 40:41–59.
- Wright, S. 1920. The relative importance of heredity and environment in determining the piebald pattern of guinea-pigs. *PNAS*, 6(6):320–332.
- Zelditch, M. 1988. Ontogenetic variation in patterns of phenotypic integration in the laboratory rat. *Evolution*, 42(1):28–41.
- Zhang, J. & Spirtes, P. 2003. Strong faithfulness and uniform consistency in causal inference. In: *Proceedings of the nineteenth conference annual conference on uncertainty in artificial intelligence* (C. Meek & U. Kjærulff, eds), pp. 632–639, Morgan Kauffmann, San Francisco, California.

Table 1: Comparison of multiple regression and the FCI algorithm under different selective scenarios where only the bottom row represents selection.  $Z_2$  is the auxiliary phenotype that is not causally adjacent to fitness. This means there exists a set  $\mathbf{S}(Z_2, W)$  conditioned on which  $Z_2$  is independent of  $W$ . The test declares selection on  $Z_1$  if  $\mathbf{S}(Z_2, W)$  includes  $Z_1$  (bottom). Note that multiple regression (second column) provides no information as to the possible confounding and falsely concludes selection on unselected trait  $Z_2$  if there is confounding.

**Figure 1**

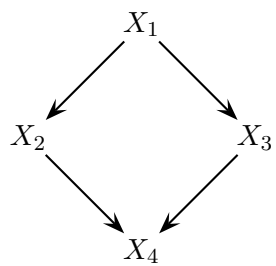


**Figure 2**

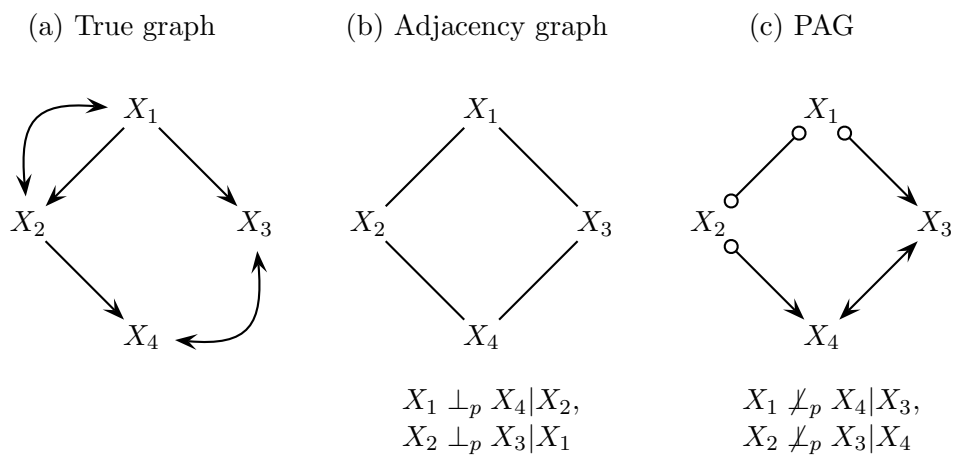
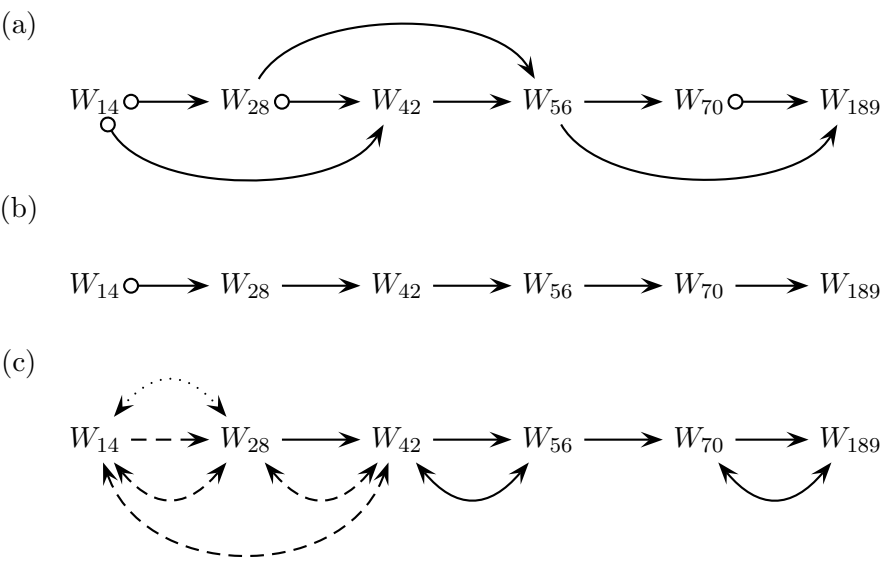
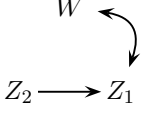
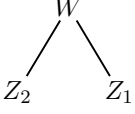
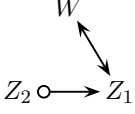
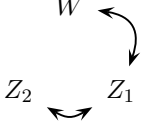
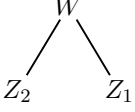
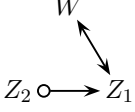
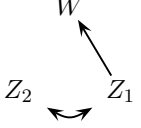
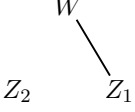
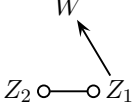


Figure 3



**Table 1**

	Truth	Regression	FCI	Independence
Confounded				$W \perp_p Z_2   \emptyset$ $(\mathbf{S}(Z_2, W) = \emptyset)$
Confounded				$W \perp_p Z_2   \emptyset$ $(\mathbf{S}(Z_2, W) = \emptyset)$
Selection				$W \perp_p Z_2   Z_1$ $(\mathbf{S}(Z_2, W) = \{Z_1\})$